

BONDED HIGH STRENGTH CONCRETE OVERLAYS EXPOSED TO AUTOGENOUS AND DRYING SHRINKAGE.

T.Kanstad
Department of Structural Engineering, University of Trondheim
Trondheim, Norway

Abstract

The behaviour of concrete slabs with bonded high strength concrete overlays exposed to shrinkage and temperature effects is investigated in an experimental and theoretical study. Development of strains with time, and the stresses at the interface between the two materials, are subjects of major interest. The theory is based on nonlinear diffusion and may be used both for early age periods where self-desiccation and temperature effects dominate and for later ages where external drying dominates. It is implemented in the nonlinear finite element program system Diana, and may be used for the most commonly used element types together with the concrete creep and crack models available in the standard version. The article reports ongoing research and it is concluded that the results obtained so far are promising.

1 Introduction

A main objective by this project is to increase the understanding of the mechanical behaviour of concrete structures with overlays exposed to

differential volume changes. In these types of structures delamination at the interface between the two materials has been a serious problem, especially after overlays of high strength concrete was introduced. The work is mainly directed toward the edge-zones where the problems usually start in practice. In Scandinavia, where most cars in the winter season use studded tires, the problem is relevant for reparation of rutted bridge decks and concrete roads.

This paper is divided into three main parts, experimental work, theory and comparisons between the results. An important part of the project is also to develop a simplified model for design purposes. This model is based on findings from the finite element analyses, but more experimental results must be studied and further parameter studies carried out before the model can be published.

2 Experiments

2.1 Slabs with bonded high strength concrete overlays

These experiments included two reinforced concrete slabs of dimension 1.5·1.5·0.3 m and 0.8·0.8·0.2 m with 70 mm thick overlays as illustrated in Fig. 1. The structural concrete had a planned mean cube strength on 45 MPa while the overlay was a typical high strength concrete with mean strength 95 MPa and a water/binder-ratio on 0.36. The overlay was applied when the structural concrete was 28 days old, and after 7 days of moist curing, the surface of the overlay was exposed to drying at RH=40% and T=20°C.

The slabs were instrumented by strain gauges at 4 different levels of the composite cross section height. This was done at three different distances from the edge at four different sections of each slab. Consequently there were 48 strain gauges in each slab which should give a reasonably good description of the strain distribution in the slabs.

Different methods of surface-preparation of the structural concrete were tried, and each slab was divided into four triangular segments. This included unprepared or lightly hammered surface, wet or dry and non-grouted or grouted surfaces. Pullout bond tests showed positive effects of light hammering and wet surface, while no significant effect of cement-latex-grouting was observed. All segments showed a considerable degree of delamination after a few months of drying.

2.2 Beams exposed to one-sided drying

In addition a series of beams illustrated in Fig. 2 (Johansen,1988), are included in this paper. The objective by this test is due to the need for simple methods for characterization of the crack sensitivity of concrete exposed to

drying. This method gives directly a time dependent curving tendency caused by one-sided drying, which also is the most important effect in the slab described above. A main reason for including these experiments in this paper, is the need for verification of the theory. The beams are simpler to analyse and the results easier to interpret than for the slab.

The beams were stored under wet burlap for 10 days and then exposed to drying at RH=50% from the top edge. In one test the beam is free to curve, and the vertical deformation (y) is measured. In the second test, the beam is fixed by a vertical force (F). Results from tests with two concrete mixes are reported in this article. The only difference is that 1% steel fiber is added in one of them. The water/binder-ratio was 0.73 and the cube strength 56 MPa after 28 days.

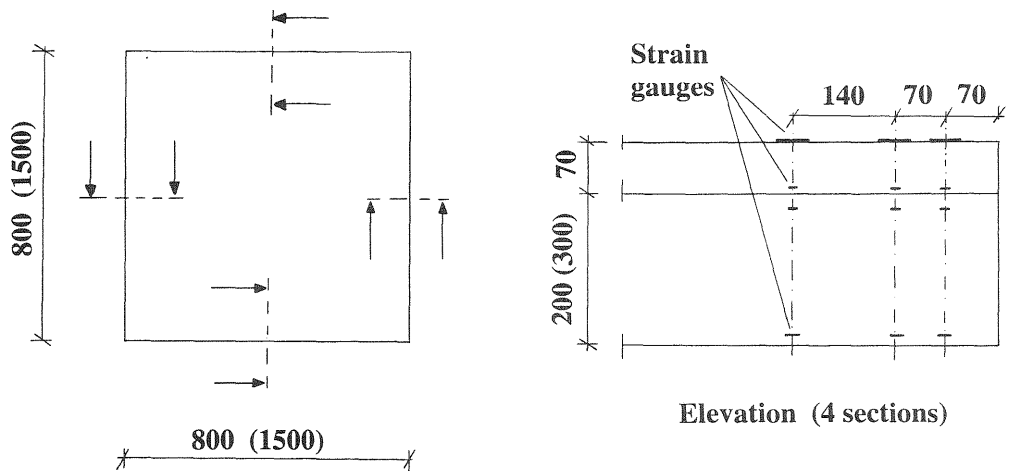


Fig. 1. Geometry of slab and location of strain gauges (Kanstad 1992).

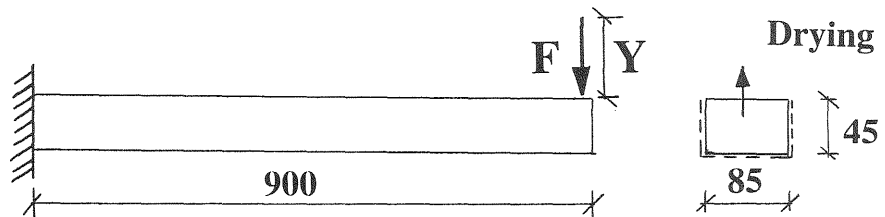


Fig. 2. Tests with beams exposed to one-sided drying (Johansen 1988)

3 Theory

3.1 General

Stress development in early age concrete and concrete exposed to drying is a complicated coupled moisture, temperature and mechanical problem. In this work, this is simplified and the only coupling between the two first and the latter problem is the initial strains caused by the volume changes.

The subsequent equations are included as a general model in Diana, and can be used together with element types as volume elements, plane stress or plane strain elements, axi-symmetric or interface elements. Consequently it is possible to analyse most types of structures. The moisture and temperature equations may also be combined with models for discrete or smeared cracking and creep based on linear viscoelasticity with aging. For time integration the Euler backwards method is used. Considering discretization of displacement-, moisture- and temperaturefields the Standard Galerkin method is used, and the capacity matrixes are lumped.

3.2 Humidity

The relative humidity inside the specimens is assumed to be governed by the following equations (Bazant and Najjar 1972):

$$\frac{\partial h}{\partial t} = \nabla(k_H \nabla h) - K \frac{\partial T}{\partial t} - \frac{\partial h_s}{\partial t} \quad (1)$$

$$k_H = C_1 \left(\alpha_0 + \frac{1 - \alpha_0}{1 + \left(\frac{1-h}{1-h_c} \right)^n} \right) \quad (2)$$

$$K = 0.0135h \frac{1-h}{1.25-h} \quad (3)$$

In these equations t represents the time, h the relative humidity, k_H the diffusion coefficient, K the hygrothermic coefficient, and h_s the self desiccation. C_1, α_0, h_c and n are material parameters.

For concretes with low water/binder-ratios self-desiccation is a significant effect, and in this work a polynomial of the equivalent time t_{eq} is used:

$$h_s = a_i t_{eq}^i \quad (4)$$

3.3 Temperature

The temperature development is governed by the general heat equation:

$$\rho C \frac{\partial T}{\partial t} = \nabla(k_T \nabla T) + \frac{\partial Q_c}{\partial t} \quad (5)$$

In which ρ is the density, C the heat capacity, k_T the thermal conductivity and Q_c the amount of produced hydration heat at that time.

The hydration process may be characterized by the maturity defined as the relative amount of accumulated heat production at time t . In this project an expression originally proposed by Byfors is used (Jonasson et al 1994):

$$\alpha = \frac{Q_c(t)}{Q_c(t=\infty)} = \exp\left(-\lambda_1 \left(\ln\left(1 + \frac{t}{t_{eq}}\right)\right)^{-\kappa_1}\right) \quad (6)$$

In which α is the maturity, λ_1 , t_1 and κ_1 are material parameters and t_{eq} is the equivalent time determined by the Arrhenius principle.

Both for the humidity and the temperature calculations special elements with convective boundary conditions to the environments are used.

3.4 Initial strains

Simple expansion relations for the humidity strain rate $\dot{\epsilon}_{sh}$ and the temperature strain rate $\dot{\epsilon}_T$ are assumed:

$$\dot{\epsilon}_T = \alpha_T \dot{T} \quad \dot{\epsilon}_{sh} = \alpha_{sh} \dot{h} \quad (7)$$

For α_T a polynomial expression of the maturity, α , is assumed since, especially in the very early phase, α_T shows a strong age dependence (f.i. Kanstad 1994). For shrinkage the expansion coefficient α_{sh} is assumed to be independent on the humidity h (f.i. Bazant and Najjar 1972).

4 Results

4.1 Drying of concrete cylinder

For verification of the diffusion theory a benchmark example is used (Espion 1993). The cylinder was sealed at top and bottom, and drying took place in radial direction only. In the analysis axi-symmetric elements were used. Calculated and experimental results are compared in Fig. 3.

4.2 Beams exposed to one-sided drying

Fig. 4 shows experimental and calculated results for the two beams in Fig. 2. The beams were modelled with plane stress elements, and divided into 50 elements over the height and 10 elements in the length direction. The length of the time steps was 1 day. Creep was included by the CEB 1990 Model Code as a cross section property, and approximated by an aging Maxwell chain model (Visschedijk 1995). The smeared crack approach was used, although the degree of cracking was low.

When comparing the results, it should be noted that this work still not is finished, and that more experimental data has to be studied and the material parameters determined with larger significance before any conclusions about the general validity of the theory can be drawn. Anyway, for the restrained beam, the deviation can partly be due to nonlinear creep effects and nonuniform creep properties over the cross section height.

4.3 Debonding of high strength concrete overlays

Fig. 5 shows temperature compensated strains versus time after casting for three different locations in the cross section. The experimental results are average values of four sections in the smallest slab (800·800 mm). The corresponding stresses showed that in this particular case, the cracking risk in the early age period is low, although the self-desiccation shrinkage is rather high for this concrete. It should be noted that an approach, alternative to the one presented in Ch. 3, is used for the early age part of this analysis (van den Boogaard et al 1994, Kanstad 1994). The main difference is due to the autogenous shrinkage which is modelled directly as a function of the maturity, α , (Mazars 1994):

$$\epsilon_{sh}(\alpha) = \epsilon_{sh\infty} \alpha (2 - \alpha) \quad (8)$$

The composite structure was modelled with plane stress elements. It was divided into 20 elements in the length direction, and 20 elements in the vertical direction both for the overlay and for the structural concrete. The interface between the two materials was modelled by interface elements and discrete cracking and linear softening. Calculated and measured strain development is compared in Fig. 6 for several locations in the composite structure. Also here the experimental results are average values of four sections in the smallest slab. It is seen that the strains at the top of the overlay decrease with increasing distance from the edge, which is explained by the effect of restraint from the structural concrete. The main reason for the deviation between the calculated and experimental results is probably due

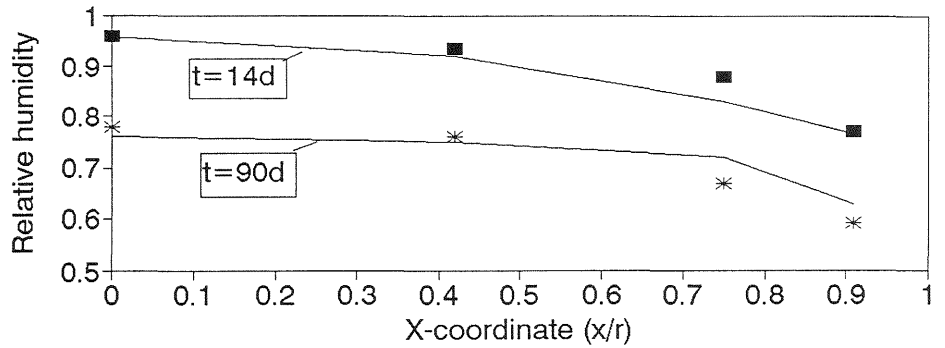


Fig. 3. Experimental and theoretical relative humidity distributions at different drying times. Cylinders with $d=152.4$ mm. $C_1=38.2$ mm²/day, $\alpha_0=0.05$, $h_c=0.75$, $n=16$. Ambient conditions $RH=50\%$, $T=23^\circ\text{C}$.

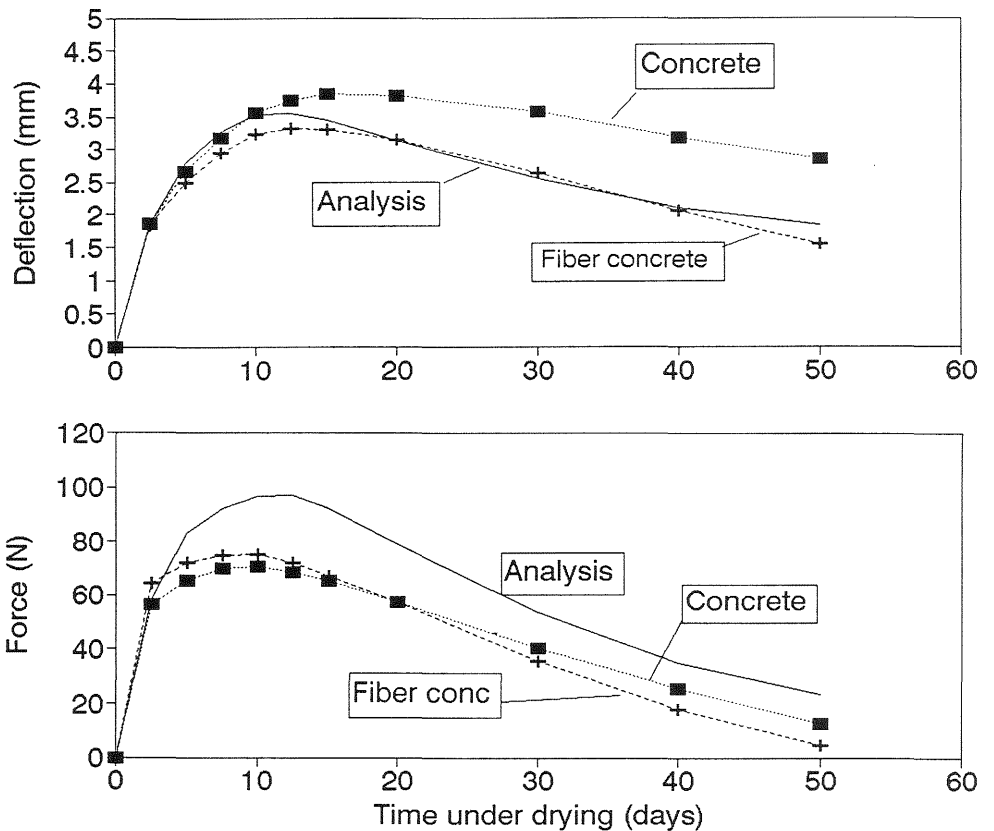


Fig. 4. Measured and calculated results for the beams in Figure 2. (a) Free beam, (b) Fixed beam, $C_1=25$ mm²/day, $\alpha_0=0.05$, $h_c=0.75$, $n=16$, $\alpha_{sh}=1.75 \cdot 10^{-3}$, $E_c=22000$ MPa, $RH=50\%$, $T=20^\circ\text{C}$, Creep Model Code 1990.

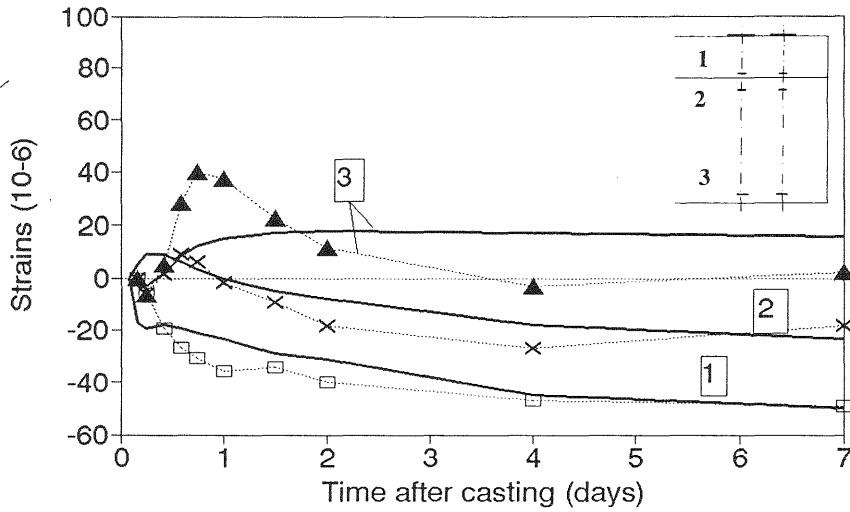


Fig. 5. Temperature compensated strains in the slabs. $\epsilon_{sh\infty} = 0.05 \cdot 10^{-3}$

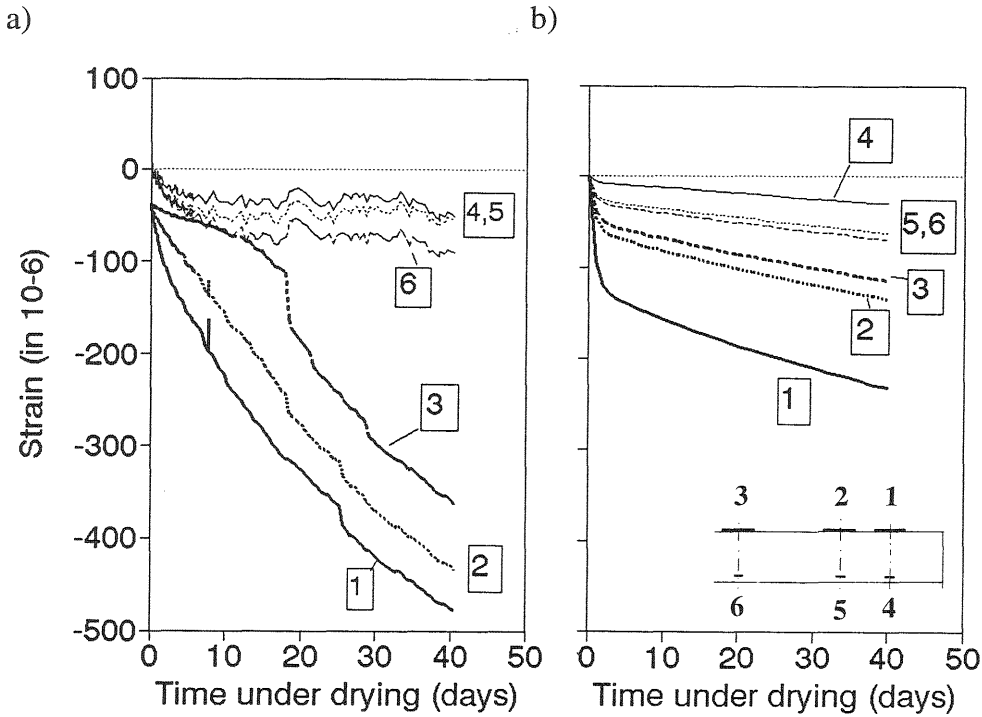


Fig. 6. Strain development in the overlay after exposure to drying. (a) Experiment, (b) Analysis. Material parameters: Overlay: $C_1 = 25 \text{ mm}^2/\text{day}$, $\alpha_0 = 0.05$, $h_c = 0.75$, $n = 16$, $\alpha_{sh} = 2.0 \cdot 10^{-3}$, $E_c = 33000 \text{ MPa}$, $\text{RH} = 40\%$, $T = 20^\circ\text{C}$. Interface: $f_t = 1.7 \text{ MPa}$, $G_f = 50 \text{ N/m}$.

to the degree of cracking at the interface between the two materials. This statement is supported by the results in Fig. 7 which shows calculated normal stresses along the interface 40 days after start of drying.

It is also important that this type of fracture is rather unstable and might be difficult to handle numerically. The analyses are very time-consuming, and so far it has not been possible to use as fine mesh as desired.

5 Conclusions and plans for further work

For structures exposed to drying and autogenous shrinkage, reasonable or promising agreement between experiments and theory is achieved by a method founded on nonlinear diffusion theory and the general differential equation for transient temperature fields.

Considering further work, the main objective is still to contribute to safer design, regarding choice of materials, overlay thickness, curing conditions and need for special surface preparation. To achieve this result, more research on material models, numerical solution methods and parameter studies or verification against experimental results remains to be done.

6 Acknowledgement

The project is financially supported by the Norwegian road department and the University of Trondheim. The author greatly acknowledge the work of D.G.Roddeman (TNO Building and Construction Research, The Netherlands) who implemented the models and carried out analyses during his post doctoral stay at the University of Trondheim in 1994-95.

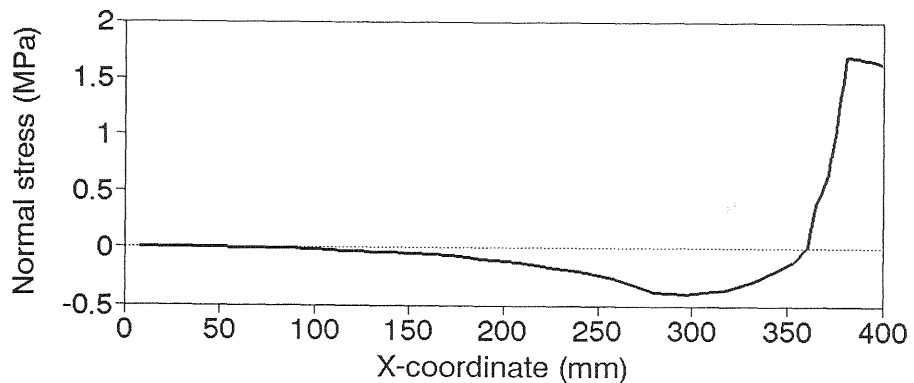


Fig. 7. Calculated normal stresses along the interface after 40 days of drying.

6 References

- Bazant, Z.P., and Najjar, L.J. (1972) Nonlinear water diffusion in nonsaturated concrete, in **Materials and Structures (RILEM)**, Vol 5, pp 3-19.
- Boogaard, A.H. van den, Borst, R.de, (1994) Finite element modelling of deformation and cracking in early-age concrete, **Journal of Eng. Mechanics, ASCE**, 120 (12), 2519-2534.
- Espion, B. (1993) Benchmark examples for creep and shrinkage analysis computer programs, in **Creep and Shrinkage of Concrete** (eds Z.P. Bazant and I. Carol), E.& F.N.Spon, London, 877-888.
- Johansen, R. and Bernhardt, C.J. (1988) Serviceability of concrete, volume changes and cracking, Sintef report no.651624.04 (in norwegian).
- Jonasson, J.E., Groth, P., and Hedlund, H. (1994) Modelling of temperature and moisture field in concrete to study early age movements as a basis for stress analysis, in **Thermal Cracking in Concrete at Early Ages**, (ed R.Springenschmid), E.& F.N.Spon, London, 45-52.
- Kanstad (1992), Concrete slabs with bonded concrete overlays exposed to drying shrinkage, Report Dep. of struct. eng., University of Trondheim.
- Kanstad (1994) Early age behaviour of concrete and reinforced concrete structures, Report Mechanics and Structures Division, TU Delft, Department of structural engineering, University of Trondheim.
- Kanstad, T., de Borst, R., and van den Boogaard, A.H. (1994) Early age behaviour of concrete and reinforced concrete structures, **Seventh Nordic Seminar on Computational Mechanics** (ed K.Bell), University of Trondheim, 198-201.
- Mazars, J. and Bournazel, J-P. (1993) A damage modelling for RCC dam and mass concrete: Initial state and evolution under loading, in **Dam Fracture and Damage** (eds. Bourdarot, Mazars and Saouma) Balkema, Rotterdam, 155-161.
- Visschedijk, M., (1995) Creep in aging concrete, TNO-memo 95, TNO Building and Construction Research, The Netherlands.